Bond slip and crack development in FRC and regular concrete specimens longitudinally reinforced with FRP or steel under tension loading

Lárusson, Lárus Helgi; Fischer, Gregor

Published in:
Proceedings of Bond in Concrete 2012

Publication date:
2012

Bond slip and crack development in FRC and regular concrete specimens longitudinally reinforced with FRP or steel under tension loading

L. H. Lárusson & G. Fischer
Department of Civil Engineering, Technical University of Denmark, Kgs. Lyngby, Denmark

ABSTRACT: The governing mechanism in the structural response of reinforced concrete members in tension is the interaction between structural reinforcement and the surrounding concrete matrix. The composite response and the mechanical integrations of reinforced cementitious members were investigated during tensile loading using high definition image analysis in two unique test setups. Two different types of cementitious materials, conventional concrete and highly ductile Engineered Cementitious Composite (ECC), and two types of reinforcement bars, regular steel and Glass Fiber Reinforcement Polymer (GFRP), were tested. It was found that the ductile ECC in contrast to regular brittle concrete decreases crack widths significantly which effectively results in decreased bond slip between the reinforcement and surrounding matrix. Furthermore the use of elastic GFRP in comparison to elastic/plastic steel reinforcement seems to increase the number of cracks forming over a longer strain interval, especially secondary cracks.

1 INTRODUCTION

1.1 *Motivation*

The research activities presented in this paper are part of a study that focuses on research and design of a continuous expansion joint, also known as link slab (Caner & Zia 1998), for roads and bridge structures. In this context, by using composite materials such as Engineered Cementitious Composites (ECC) and Glass Fiber Reinforced Polymer (GFRP) rebars, the aim of this study is to improve the performance, the production process and applicability as well as durability of current expansion joints.

1.2 *Materials and compositions*

ECC is a subclass of High Performance Fiber Reinforced Cementitious Composite (HPFRCC) (Naaman 2006), which has the ability to exhibit strain hardening with a relatively high strain capacity through the formation of multiple cracking accompanied by limited crack widths (<250 μm @ 4.0% strain). To contrast the highly ductile behavior of ECC, a series of conventional concrete specimens with the same compression strength as ECC were also evaluated.

The GFRP reinforcement used in this study (Aslan-100 produced by Hughes Brothers inc.) is a sand coated, relatively low E-modulus, elastic, corrosion free alternative to regular steel reinforcements. For comparison purposes regular elastic-plastic steel reinforcement was included in the composite test series.

The experimental programs presented in this paper focus on the interactions of reinforced cementitious composite in direct tension. The test series carried out examine four different material compositions: steel reinforced concrete (R/C) steel reinforced ECC (R/ECC), GFRP reinforced concrete (GFRP/C) and GFRP reinforced ECC (GFRP/ECC).

All test configurations were subject to direct monotonic tensile loading in two different test setups: (i) The tension stiffening setup focused on the tension stiffening process, crack formation and development, crack widths and crack spacing. (ii) The interface setup focused on the rebar-matrix interface, specifically on the degradation of the rebar-matrix interface during tensile loading.

The four structural materials investigated in this study were tested individually to establish their material properties. Table 1 shows the parameters obtained. Conventional concrete and ECC were tested in compression while ECC, regular steel and GFRP reinforcement were tested in direct tension.

Tabel 1: Material parameters. f_{cu} and ε_{cu} refer to the ultimate compression strength and strain, f_t is the tensile strength, ε_{ty} and ε_y are the tensile strains at yielding, f_y is the tensile yield strength, f_{tu} is the ultimate tensile strength and ε_{tu} is the ultimate tensile strain.

	f_{cu} [MPa]	ε_{cu} [%]	f_t [MPa]	ε_{ty} [%]	E [GPa]
Concrete	61	0.12	4.1*	-	38
ECC	60	0.22	3.5**	0.03	16
	f_y [MPa]	ε_y [%]	f_{tu} [MPa]	ε_{tu} [%]	E [GPa]
Steel rebars	680	0.35	780	6.9	202
GFRP rebars	-	-	1050	2.7	46

* Value obtained from a split cylinder test (EN 12390-6:2009).
** First crack strength, ultimate strength reached 4.0-4.5 MPa at about 2.0-4.0 % strain.

2 CONCEPT

The tension stiffening process of reinforced concrete elements in direct tension is governed by the mechanical fracture properties of the bond between rebar and concrete and the material properties of both concrete and reinforcement (Fischer & Li 2004). In this context the tension stiffening phenomenon is usually defined as the difference between the response of the bare reinforcement and the composite element during tensile loading, either in bending or in direct tension. Consequently, tension stiffening is a measurement of the degradation of the rebar-matrix interface.

By introducing a ductile cementitious composite such as ECC into a reinforced element the supplementary strain and tensile load capacity of the ECC can be utilized. In addition to the load and ductility enhancements the benefits of closely spaced multiple cracking with measurably reduced crack widths, in comparison to conventional brittle concrete, results in less deterioration of the composite behavior (decreased bond slip) and increased durability of the structure.

To emphasize the difference between reinforced concrete and reinforced ECC (or any other HPFRCC) in direct tensile loading, schematic illustrations are given in Figure 1. It is noted that GFRP reinforced members in direct tension exhibit the same respond as is illustrated in Figure1 up to yielding (region 1-3).

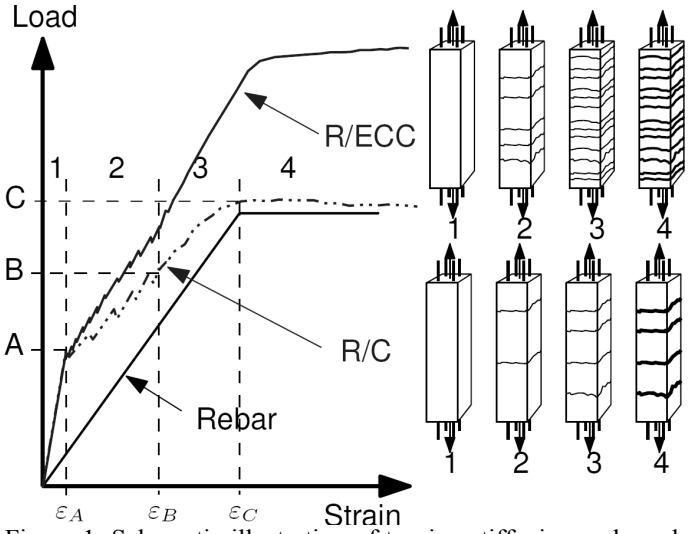

Figure 1: Schematic illustration of tension stiffening and crack formation for R/C and R/ECC. "A" and ε_A are load and corresponding strain of first crack respectively, "B" and ε_B are load and strain after crack saturation respectively, "C" and ε_C are load and strain at yielding of reinforcement respectively.

3 EXPERIMENTAL PROGRAMS

3.1 *Tension stiffening setup*

In the tension stiffening setup twelve composite specimens with identical geometry, three for each composition, were prepared and tested. The dog bone shaped specimens were 1000 mm long with a 500 mm long middle section with a constant cross section: 100 x 100 mm^2 and four rebars positioned equally in the cross section (Fig. 2). The rebars extended throughout the entire length of the specimens, protruding from both ends. The diameter of the four rebars were Ø 6 mm resulting in a reinforcement ratio ρ = 1.14 % for the steel reinforced member and ρ = 1.28% for the GFRP reinforced members (as the cross section area of the GFRP bars was slightly larger than that of the steel bars).

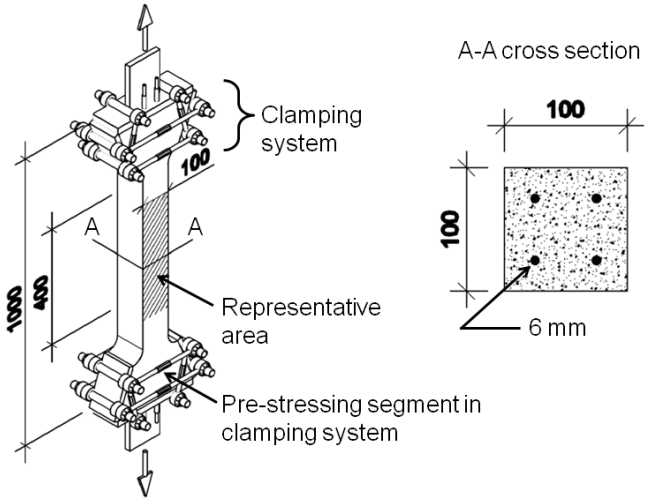

Figure 2: Test configuration with a clamping system located on both ends to ensure a composite behavior of the representative section. The cross section of the representative section is also shown.

A digital image correlation was utilized to measure surface displacements and quantitative crack opening information of the specimens during testing. The measured surface area was approximately 250 mm along the specimens length and 100 mm wide. Furthermore two LVDT´s were also positioned on each side of the representative surface area, 400 mm apart, to obtain more detailed deformation information of the whole representative section (see Fig. 2). All tests were carried out in a displacement controlled loading sequence with a monotonic loading rate of 0.5 mm per min. Specimens were loaded up to approximately 1.2 % tensile.

3.2 *Interface setup*

For the interface test setup twelve reinforced prisms with identical geometry were also prepared and tested, three for each composition.

The 400 mm long, 100 mm wide and 35 mm thick prisms where designed with a reduced width at the mid section (Fig. 3). At the mid section a 50 mm stretch the concrete was removed on each side of the reinforcement, reveling the longitudinal reinforcement slightly. This unique configuration allows for the rebar-matrix interface to be viewed and consequently analyzed using image correlation during testing (Fig. 4).

The Ø 6 mm rebars extended throughout the entire length of the specimens and were secured to a steel plate at both ends. The representative cross section resulted in a reinforcement ratio ρ = 2.7 % for the steel reinforced members and ρ = 3.0 % for the GFRP reinforced members.

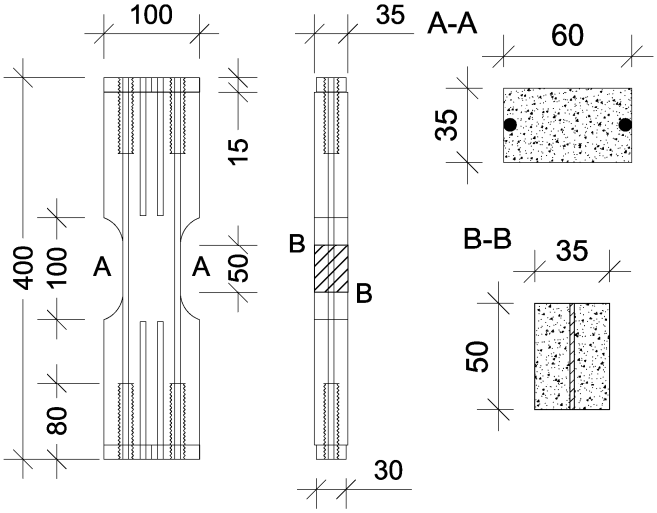

Figure 3: Geometry and layout of reinforced prism (interface setup) used to evaluate the rebar-matrix interface in tensile loading.

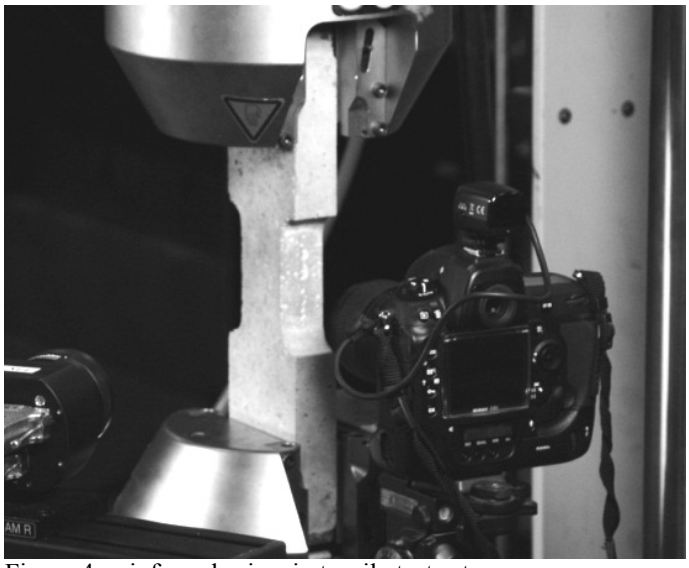

Figure 4: reinforced prism in tensile test setup.

With the partially exposed rebar on the measured representative surface (see B-B in Fig. 3) and utilizing the image correlation analysis, a single crack was monitored as it initialized and developed during loading. The first crack observed in each specimen was chosen and analyzed in detail from the outer surface to the rebar-matrix interface. Furthermore, the slip along the rebar-matrix interface (as a result of the transverse crack) was measured as well.

Figure 5 shows an example of a strain simulation of the measured area of an R/C specimen. The zoomed-in box shows the first transverse crack and the resulting debonding zone along the length of the longitudinal rebar. The first crack was chosen for analysis to minimize the effects of surrounding cracks and crack branching.

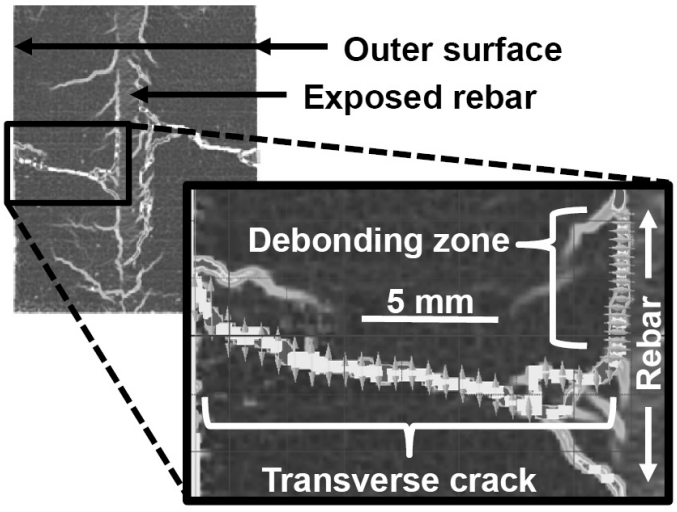

Figure 5: Example of image correlation analysis, lighter colored areas depict strain intensities (indicating a crack/slip) on the measured representative surface area being monitored (see B-B in Fig. 3 and Fig. 4).

4 RESULTS

4.1 *Tension stiffening setup*

Figure 6 shows the structural response of steel reinforced ECC and steel reinforced concrete specimens in monotonic tensile loading.

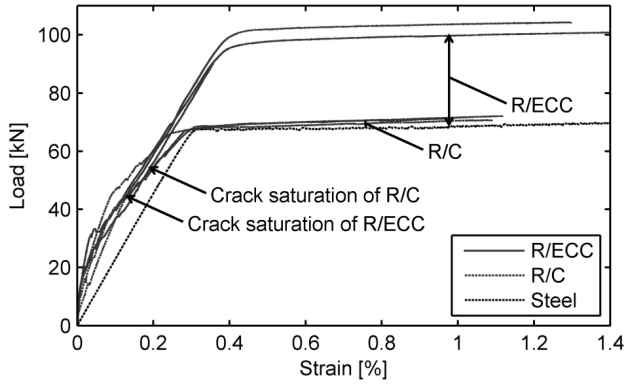

Figure 6: Structural response of R/C and R/ECC specimens during monotonic tensile loading. The tension stiffening effect for both compositions are indicated on graph.

In accordance with the different response phases schematically illustrated in Figure 1, the following parameters are obtained from results shown in Figure 5 and Figure 6.

The first crack load levels of the composites differ somewhat between specimens of all compositions types, due to minor miss-alignment observed in the test configuration causing transverse cracking to occur at lower tensile loads than expected.

The first cracking in R/ECC specimens is reached at an approximate strain level of 0.01-0.02 %, corresponding to a load of 10-30 kN. After crack saturation is reached at about 0.09 % strain, the load-strain response of the specimen is linear until yielding of the reinforcement commences at 0.3-0.35 % strain corresponding to 93-98 kN tensile load. Finally, the monotonic tensile loading was discontinued at 1.1-1.3 % strain, corresponding to a tensile load range of 99 kN to 104 kN.

Strain and corresponding load values for all composition types are presented in Table 2.

Initially, the response of R/C is similar to that of R/ECC but as the strain level increases, the stiffness of the composite decreases, which means that the tension stiffening diminishes with increased loading. After yielding of the reinforcement the concrete composite response is only slightly higher than that of the bare rebar as shown in Figure 5.

The load-strain response of GFRP/ECC and GFRP/C is displayed in Figure 7 together with the response of bare GFRP rebar. GFRP/ECC exhibits crack formation up to about 0.4 % strain after cracking initiated. Beyond crack saturation the stiffness of the composite specimens increases again, showing a slightly stiffer response than the bare GFRP rebar (see Fig. 7).

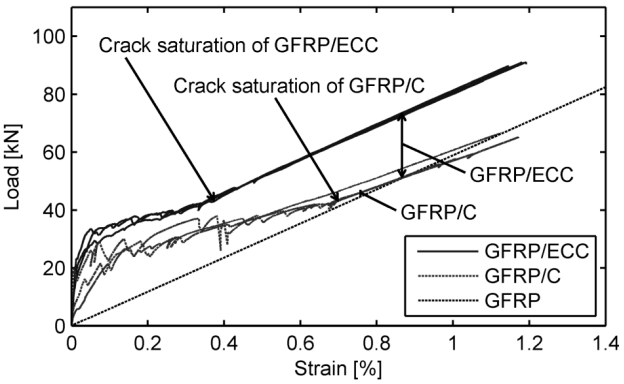

Figure 7: Structural response of GFRP/C and GFRP/ECC specimens during monotonic tensile loading. The tension stiffening effect for both member types are indicated on graph.

Tabel 2: Experimentally obtained values from tensile loading of tension stiffening setup specimens

	First crack		Crack saturation		Rebar yielding	
	Strain	Load	Strain	Load	Strain	Load
	[‰]	[kN]	[‰]	[kN]	[‰]	[kN]
R/C	0.1-0.3	14-18	1.5-2	50-66	3-3.5	68
R/ECC	0.1-0.2	10-30	0.9	30-40	3-3.5	93-98
GFRP/C	0.1-0.3	5-20	4-7	35-42	-	-
GFRP/ECC	0.1-0.3	16-21	4-4.5	40-42	-	-

Coefficients were assessed from Figure 3 and Figure 5 according to Figure 1.

The GFRP/C specimens show a similar behavior to the GFRP/ECC specimens up to about 0.4 % strain but at lower load levels (see Fig. 6). After crack saturation, the composite stiffness is slightly lower than that of the GFRP alone.

Figure 7 and Figure 8 show strain intensities (indicating a crack) on the representative surfaces of the specimens using the image correlation analysis. In Figure 7 and 8, a comparison is shown at tensile strain levels from 0.2 % to 1.0 %.

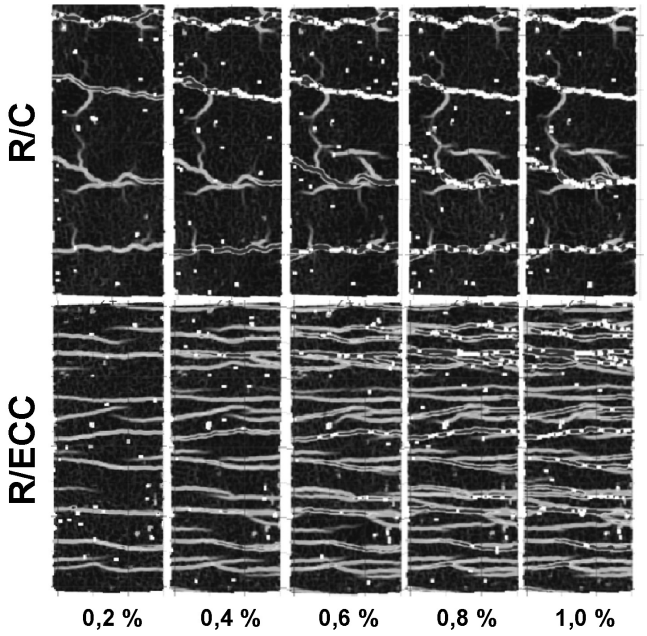

Figure 8: Crack development for R/C and R/ECC during tensile loading at strain levels 0.2-1.0 %.

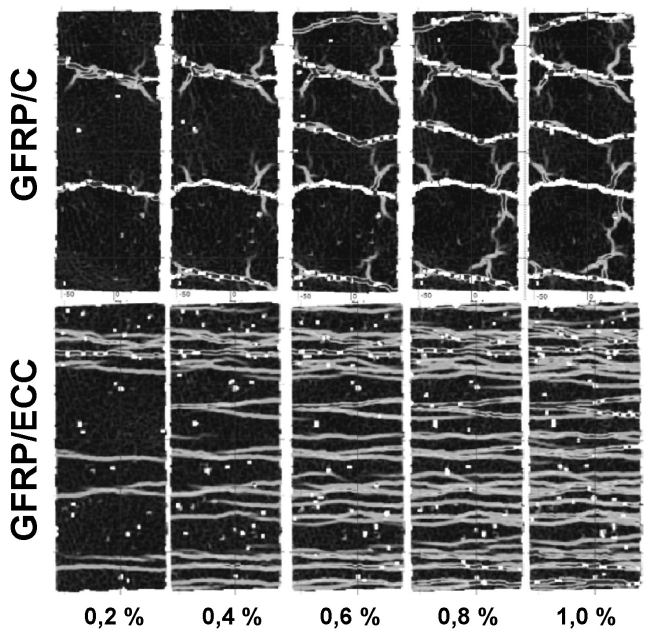

Figure 9: Crack development for GFRP/C and GFRP/ECC specimens during tensile loading at strain levels 0.2-1.0 %.

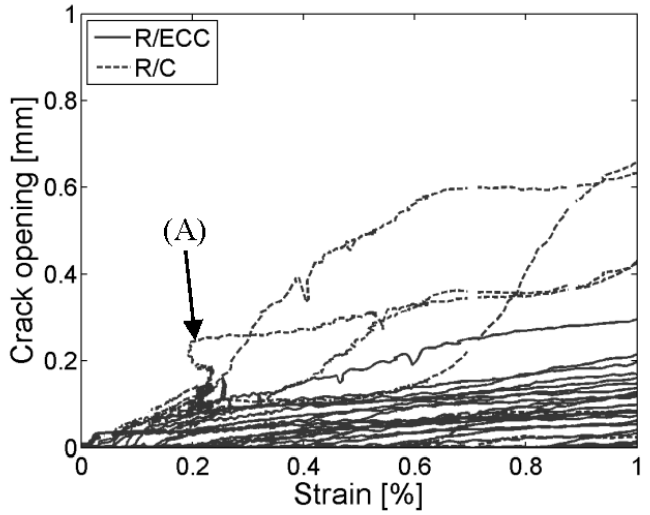

Figure 10: Development of crack opening vs. strain on R/C in comparison to R/ECC, (A) indicates where stain is halted in a R/C crack due to formation or development of another crack.

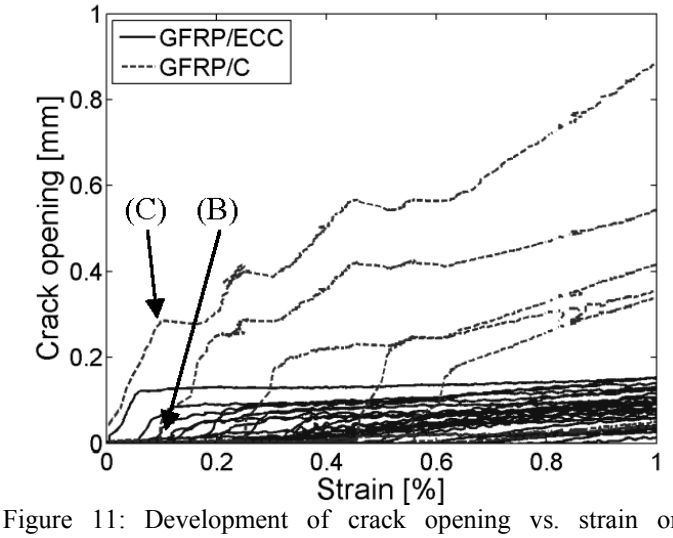

Figure 11: Development of crack opening vs. strain on GFRP/C in comparison to GFRP/ECC. (B) shows where a new crack is formed in GFRP/C while (C) indicates where crack opening is suspended due to the new crack depicted in (B) .

Furthermore, the crack opening development obtained from the image correlation analyses are shown in Figure 9 and Figure 10 as a function of strain. Crack measurements are shown for all cracks on one representative specimen of each type.

4.2 *Interface setup*

Figures 12-15 show crack width profiles for all composition types from the outer surface of the concrete to the rebar interface (Fig. 5) at different strain levels.

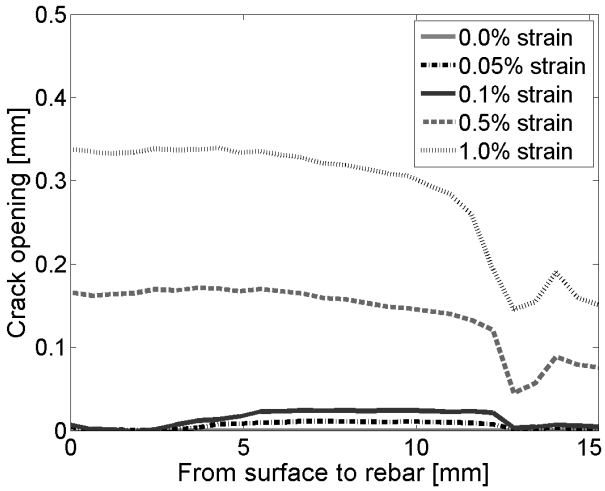

Figure 12: Crack opening profile for the first transverse crack in a R/C specimen at different strain levels.

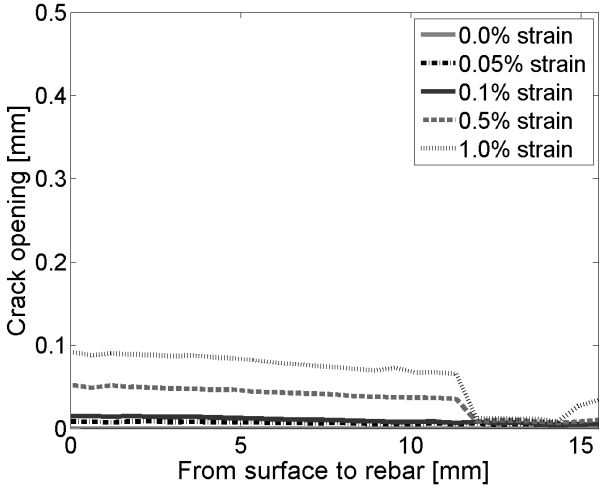

Figure 13: Crack opening profile for the first crack in a R/ECC specimen at different strain levels.

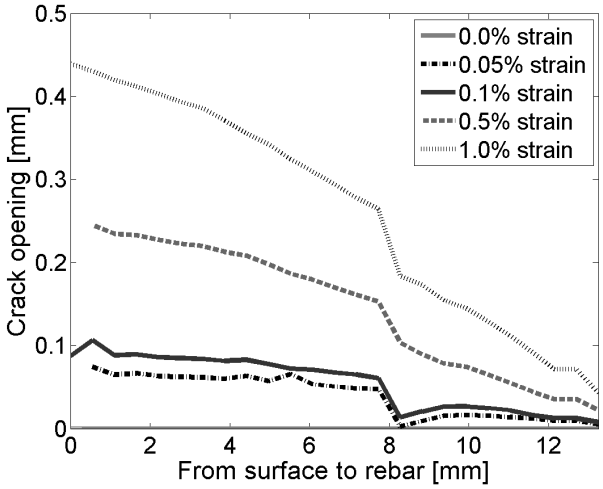

Figure 14: Crack opening profile for the first crack in a GFRP/C specimen at different strain levels.

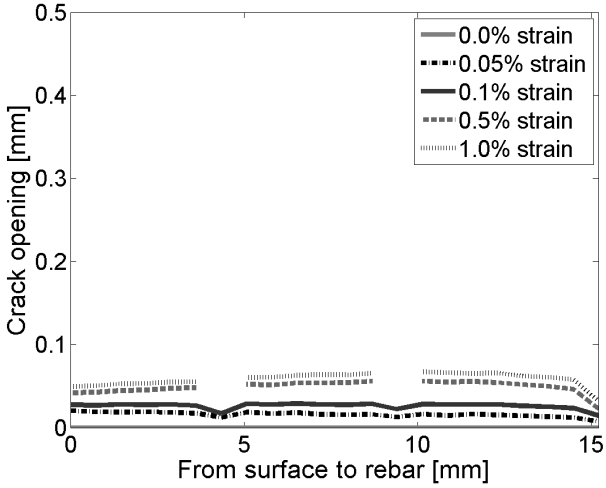

Figure 15: Crack opening profile for the first crack in a GFRP/ECC specimen at different strain levels.

Figures 16-19 show slip measurements for all composition types along the rebar at different strain levels. Measurements are initiated at the intersection of the transverse crack and the rebar-matrix interface and discontinued once the debonding reaches a second transverse crack (usually a secondary crack) at a strain level around 0.1 %.

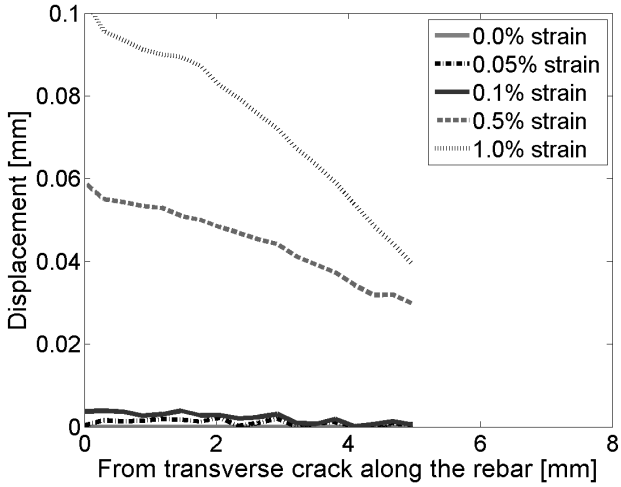

Figure 16: R/C specimen, bond slip measurements for different strain levels along the rebar length, starting at the location of the transverse crack.

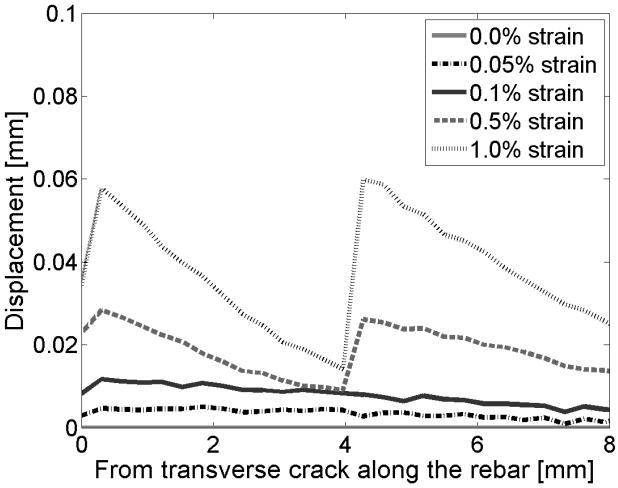

Figure 17: R/ECC specimen, bond slip measurements for different strain levels along the rebar length, starting at the location of the transverse crack.

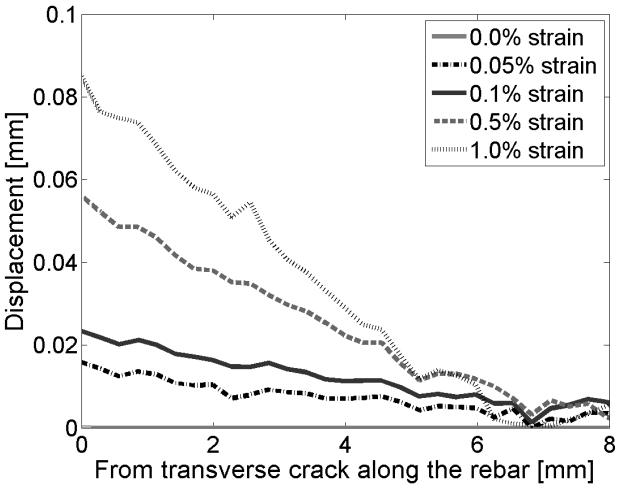

Figure 18: GFRP/C specimen, bond slip measurements for different strain levels along the rebar length, starting at the location of the transverse crack.

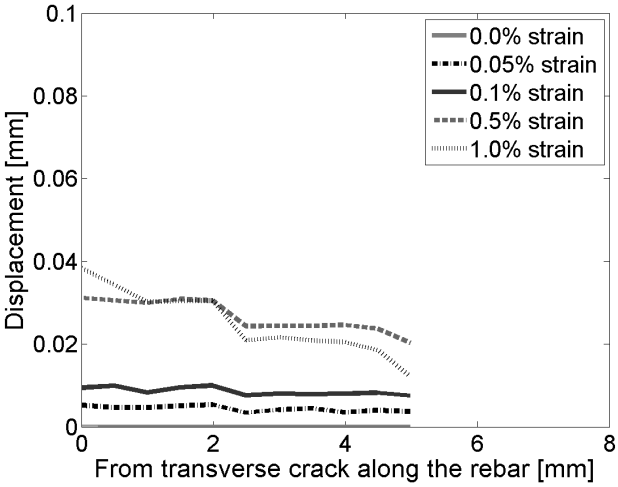

Figure 19 GFRP/ECC specimen, bond slip measurements for different strain levels along the rebar length, starting at the location of the transverse crack.

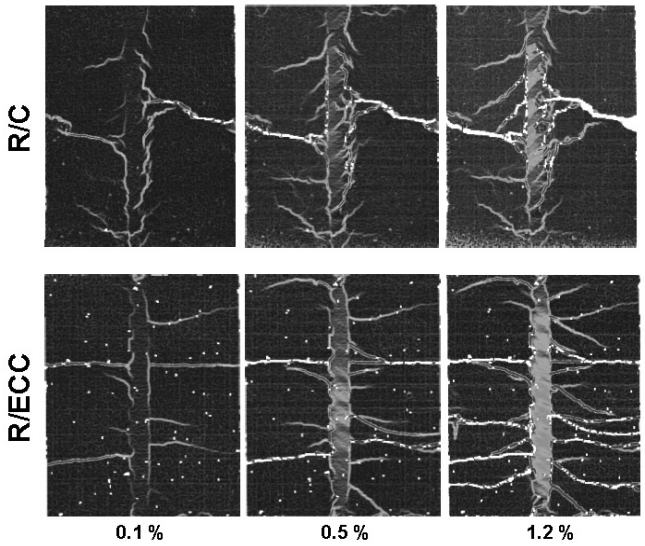

Figure 20: Crack development for R/C and R/ECC during tensile loading at strain levels 0.1-1.2 %.

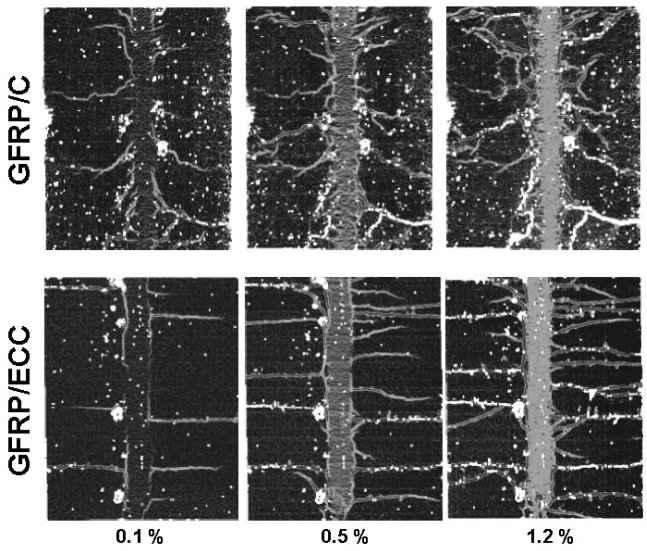

Figure 21: Crack development for GFRP/C and GFRP/ECC during tensile loading at strain levels 0.1-1.2 %.

5 DISCUSSION

5.1 *Composite response, tension stiffening setup*

Comparing the tensile loading response of reinforced concrete members to that of reinforced ECC members illustrates the additional load bearing capacity exhibited by ECC. This is seen in Figure 6 and Figure 7 as the difference between the load levels of reinforced ECC and the bare reinforcement, particularly in the post-yielding phase of R/ECC, whereas the load carrying capacity of reinforced concrete members decreases towards the capacity of the reinforcement alone. Furthermore, the stiffness of the reinforced ECC members is shown to be as high (R/ECC) or slightly higher (GFRP/ECC) than that of the bare reinforcement after crack saturation is reached. This indicates that in the tension stiffening process the contribution of ECC is maintaining the immense load response while tension stiffening in the reinforced concrete members diminishes with increasing deformations.

Initially, the influence of GFRP on the composite response is observed as crack formation occurring over a longer strain interval, i.e. crack saturation is reached at higher strain levels than for steel reinforced members, at about 0.7 % compared to 0.2 % strain respectively (see Figs. 6-7). Secondly, the tension stiffening effect in GFRP reinforced members is shown to be slightly lower than that of steel reinforced members in the post-yielding region.

However, it is noted that the shrinkage effect in reinforced tensile members needs to be accounted for to accurately evaluate the tension stiffening (Bischoff 2001).

5.2 *Crack behavior, tension stiffening setup*

Crack formation and development in reinforced ECC tension stiffening test members differ substantially from that of reinforced concrete members as shown in Figures 8-11. For the R/ECC specimen (Fig. 10), most of the cracks initiate at lower strain level (below 0.15 %) whereas the GFRP/ECC specimen (Fig. 11) develops cracks over an extended strain interval. At 1.0 % strain, both ECC composition types show approximately the same maximum crack width of 0.20 mm (Figs. 10-11). However, the GFRP/ECC specimen exhibits slightly more cracks than the R/ECC specimen resulting in an average crack spacing of 13 mm as opposed to 14.5 mm respectively. Furthermore when comparing the two ECC compositions, a slightly larger initial crack opening is seen in the GFRP/ECC member due to the lower stiffness of GFRP as opposed to the higher stiffness of the steel reinforcement.

The crack formation of the R/C specimen shows most cracks initiating at low stain levels (below 0.02 %)(Fig. 11), while the GFRP/C member initiates cracks more gradually (up to 0.6 % strain)(Fig. 11). The average crack spacing for R/C was 70 mm while GFRP/C exhibited a slightly more cracks resulting in a lower crack spacing of 60 mm.

In Figure 10, the deformation increase is momentarily halted, marked as “(A)” for the R/C specimen, indicating that cracking is forming outside of the measured area. In Figure 11 when a new crack forms in the GFRP/C specimen, depicted as “(B)”, the increasing crack opening of the pre-existing crack is suspended, marked as “(C)”, while the new crack opens up. This mechanism is observed for all composition types but is more visible in reinforced concrete members, especially the GFRP/C specimen due to the low stiffness of GFRP.

5.3 *Crack behavior, interface setup*

It is apparent from Figures 12-14 that crack widths at the outer surface of the concrete and ECC matrix

are larger than at the rebar-matrix interface. However the GFRP/ECC crack profile in (Fig. 15) shows a slightly wider crack width closer to the rebar-matrix interface, at about 10 mm from the outer surface.

The reinforced ECC specimens exhibited significantly smaller crack widths, as was expected, and indicate that the crack widths will not increase drastically with a larger cover layer (approximately 15 mm here). The reinforced concrete specimens however indicate that the crack width will grow substantially with increased concrete cover thickness. It was observed that the decrease in crack width near the rebar-matrix interface is due to branching which is more substantial in concrete specimens. This can be seen in Figures 12-14 as sudden drops in crack widths as the crack profile gets closer to the rebar-matrix interface. The homogeneous crack widths observed throughout the crack profiles of reinforced ECC members are a result of the fiber bridging which limits the crack width as well as transfers load through the section.

Smaller bond-slip measurements were obtained in reinforced ECC specimens than in reinforced concrete specimens, this is seen in Figures 16-19.

As an example of the conjunction between cracks, Figure 17 shows a second crack intercepting the measured debonding length at approximately 4 mm distance from the transverse crack, causing the slip measurements to increase significantly after 0.1% strain.

In Figures 20-21, a network of secondary cracks can be seen forming and developing. Most secondary cracks in steel reinforced members initiate at the ribs of the deformed reinforcement. In reinforced concrete members these internal cracks rarely reach the outer surface, but rather propagate towards the primary cracks.

Crack spacings in reinforced ECC specimens from the tension stiffening tests (13-14.5 mm) are slightly larger than those obtained in the interface test setup (9-12.5 mm), indicating that fewer transverse cracks reach the outer surface if cover thickness is increased, either due to cracks converging or fading out before reaching the surface.

It was observed that most of the transverse cracks intercept the rebar at an angle and as a result the debonding zone tends to propagate to one side of the transverse crack depending on the angle (see Figs. 20-21). However, this process becomes less clear as branching increases and the mesh of cracks close to the rebar becomes more complicated (especially in concrete specimens).

6 CONCLUSION

To summarize the main findings of this experimental work, the following aspects can be emphasized:

- The comparison of reinforced ECC and reinforced concrete has shown that the tension stiffening process can be significantly improved by utilizing ECC.
- ECC was shown to increase the stiffness of the composite and maintaining linear stiffness throughout testing.
- The cracking process of reinforced ECC consistently showed multiple cracking with considerably smaller crack widths than those in reinforced concrete
- GFRP reinforced specimens showed larger number of cracks forming when compared to steel reinforced members, i.e. closer crack spacing.
- Comparison between the measured crack widths from the composite tests (tension stiffening setup) shows a good agreement with the test results obtained from the interface test setup when the difference in clear cover thickness is taken into account.
- The tensile stress-strain behavior of ductile ECC and low E-modulus GFRP are shown to be compatible resulting in a strong composite interaction.
- The unique test setup proposed (interface test setup) allows the measurement of the crack profile and debonding, furthermore it gives insight into the conjunction of crack networks found in reinforced members.

REFERENCES

Bischoff, P. , 2001, Effects of shrinkage on tension stiffening and cracking in reinforced concrete, *Canadian Journal of Civil Engineering*, 28, 363-374

Caner, A., Zia, P. 1998. Behavior and Design of Link Slab for Jointless Bridge Decks. *Precast Concrete Institute Journal*. May-June. pp.68-80

Fischer, G., Li, V. 2002. Influence of matrix ductility on tension-stiffening behavior of steel reinforced ECC. *ACI Structural Journal, American Concrete Institute*, 99, pp.104-111

Naaman, A., Reinhardt, H. 2006. Proposed classification of HPFRC composites based on their tensile response. Materials and Structures. Volume 39, Number 5, pp.547-555